Full-Duplex Radio for Uplink/Downlink Transmission with Spatial Randomness

Mohammadali Mohammadi[†], Himal A. Suraweera[§], Ioannis Krikidis[‡], and Chintha Tellambura[*]

[†]Faculty of Engineering, Shahrekord University, Iran (e-mail: m.a.mohammadi@eng.sku.ac.ir)
[§]Department of Electrical and Electronic Engineering, University of Peradeniya, Sri Lanka (e-mail: himal@ee.pdn.ac.lk)
[‡]Department of Electrical and Computer Engineering,University of Cyprus, Cyprus (e-mail: krikidis@ucy.ac.cy)
[*]Department of Electrical and Computer Engineering, University of Alberta, Canada (e-mail: chintha@ece.ualberta.ca)

Abstract—We consider a wireless system with a full-duplex (FD) access point (AP) that transmits to a scheduled user in the downlink (DL) channel, while receiving data from an user in the uplink (UL) channel at the same time on the same frequency. In this system, loopback interference (LI) at the AP and inter user interference between the uplink (UL) user and downlink (DL) user can cause performance degradation. In order to characterize the effects of LI and inter user interference, we derive closed-form expressions for the outage probability and achievable sum rate of the system. In addition an asymptotic analysis that reveals insights into the system behavior and performance degradation is presented. Our results indicate that under certain conditions, FD transmissions yield performance gains over half-duplex (HD) mode of operation.

I. INTRODUCTION

Due to the exponential growth of wireless traffic, spectral efficiency improvements achievable from transmitting while receiving are highly beneficial [1], [2]. Traditionally, this was achieved by the separation of the transmit and receive carrier frequency. However, if a wireless radio node can only transmit or receive at a given time and frequency, a loss of efficiency from a channel resource perspective must be expected. A promising solution that can be employed to avoid the loss of spectral efficiency is the full-duplex (FD) technology [3]–[7].

Since the loopback interference (LI) caused by a node that is both transmitting and receiving at the same time can be overwhelming, up until now FD operation was considered practically unrealistic. This perception has been challenged due to the recent advances in antenna design and analog/digital signal processing. To this end, several recent works have described single and multiple antenna FD system designs largely made possible through new LI cancellation techniques [3], [6], [8]. The implementation of single antenna FD technology with LI cancellation was demonstrated in [3]. A multiple-input multiple-output (MIMO) FD implementation (MIDU) was presented in [6], while [7] reported design and implementation of an in-band WiFi-PHY based FD MIMO system. In [8] a massive MIMO FD relay system with spatial LI mitigation and optimum power allocation was investigated.

An interesting application of FD communications is simultaneous uplink and downlink transmission in wireless systems such as WiFi and cellular networks [7], [9], [10]. However, such transmissions introduce LI and internode interference in the network as downlink transmission will be affected by

the LI and the uplink user will interfere with the downlink reception. Therefore, in the presence of such interference, it is not clear whether FD applied to uplink/downlink user settings can bring performance benefits. In order to answer this question, several works in the literature have presented useful results. In [9] a FD cellular analytical model based on stochastic geometry was used to derive the sum capacity of the system. However, [9] assumed perfect LI cancellation and therefore, the effect of LI is not included in the results. In [11] the combination of FD and massive MIMO was considered for simultaneous uplink/downlink cellular communication. The information theoretic study presented in [12], has investigated the rate gain achievable in a FD uplink/downlink network with internode interference management techniques. The application of FD radios for a single small cell scenario was considered in [13]. Specifically in this work, the conditions where FD operation provides a throughput gain compared to HD and the corresponding throughput results using simulations were presented. In [14], joint precoder designs to optimize the spectral and energy efficiency of a FD multiuser MIMO system were presented. However [11], [12], [14] considered fixed user settings for performance analysis and as such the effect of interference due to distance, particularly relevant for wireless networks with spatial randomness, is ignored.

In this paper, we consider a wireless network scenario in which a FD infrastructure node is communicating with half-duplex (HD) spatially random user terminals to support simultaneous uplink and downlink transmissions. Our contributions are summarized as follows:

- We take both LI and inter user inference into account and derive exact expressions for the outage probability and achievable sum rate of the system. Moreover, to highlight the system behavior and shed insights into the performance degradation, an asymptotic analysis is also presented.
- We have compared the sum rate performance of the system for FD and HD modes of operation at the AP to elucidate the signal-to-noise ratio regions where the former mode of operation outperforms the latter mode of operation. Moreover, our results indicate that different power levels at the AP and UL user has a significant adverse effect to lower the sum rate in the HD mode of operation than the FD counterpart.

II. SYSTEM MODEL

Consider a single cell wireless system with an access point (AP), where data to the users in the DL channel, and data

from users in the UL channel are transmitted and received at the same time on the same frequency. All users are located in a circular area with radius R_c and the AP is located at the center. We assume that users are equipped with a single antenna, while the AP is equipped with two antennas (one antenna is used to transmit in the DL channel while the other antenna is used for UL channel reception). In the sequel we use subscript-u for the UL user, subscript-d for the DL user, and subscript-a for the AP. Similarly, we will use subscript-aa, subscript-ad, subscript-ud, and subscript-ua to denote the AP-to-AP, AP-to-DL user, UL user-to-DL user, and UL user-to-AP channels, respectively.

Let Φ_d be a two-dimensional homogeneous Poisson point process (PPP) with density λ_d that characterizes the spatial distribution of the DL users over $\mathbb{R}^2$. To obtain the most essential features, we consider the widely used Poisson bipolar model [15] and assume that the UL users are located at a fixed distance d in a random direction of angle θ from the DL users. The results obtained thus can be interpreted as the performance of networks with random link distances conditioned on the link distance having a certain value. The AP selects a DL user that is physically nearest to it. We use the terms "nearest DL user" and "scheduled DL user" interchangeably throughout the paper to refer to this user. In next generation ultra-dense networks, each user will be in the coverage area of an AP and can be considered as a most nearest user [16]. Selection of a nearest user also serves as a practical consideration for FD implementation since transmitting very high power signals towards distant periphery users in order to guarantee a quality-of-service can cause overwhelming LI at the receive side of the AP. Moreover, as a benchmark comparison we also consider the random user selection (RUS) in Section IV. In RUS method the AP randomly selects one of all candidate DL users with equal probability.

We assume that the links in the network experience both large-scale path loss effects and small-scale Rayleigh fading phenomenon. For the large-scale path loss, we assume the standard singular path loss model, $\ell(x, y) = \|x - y\|^{-\alpha}$, where $\alpha \geq 2$ denotes the path-loss exponent and $\|x - y\|$ is the Euclidean distance between two nodes.

The received power at a typical DL user located at point x_d from the AP is $P_a h_{ad} \ell(x_d)$. It is worth mentioning that the scheduled UL user, located at x_u, is served by receive antenna from AP at the same time, and it lacks coordination with concurrent active DL users. Therefore, the signal-to-interference-plus-noise ratio (SINR) of the typical DL user associated with the AP can be expressed as

$$\mathsf{SINR_d} = \frac{P_a h_{ad} \ell(x_d)}{P_u h_{ud} \ell(x_u, x_d) + \sigma_n^2}, \tag{1}$$

where P_u denotes the transmit power of the UL user in UL channel and σ_n^2 is the constant additive noise power. On the other hand, received power at the AP from the active UL user is $P_u h_{ua} \ell(x_u)$. Due to the FD mode of operation, the receive antenna of the AP will receive a LI from its transmit antenna. Hence, the resulting SINR expression at the AP can be written as

$$\mathsf{SINR_a} = \frac{P_u h_{ua} \ell(x_u)}{P_a h_{aa} + \sigma_n^2}, \tag{2}$$

where h_{aa} denotes the LI channel at the AP. In order to mitigate the adverse effects of self-interference on system

performance, an interference cancellation scheme (i.e. analog/digital cancellation) can be used at the AP and we model the residual LI channel with Rayleigh fading assumption since the strong line-of-sight component can be estimated and removed [4], [5], [17]. Since each implementation of a particular analog/digital LI cancellation scheme can be characterized by a specific residual power, a parameterization by h_{aa} satisfying $\mathbb{E}\left\{|h_{aa}|^2\right\} = \sigma_{aa}^2$ allows these effects to be studied in a generic way [17], [18].

In order to facilitate the ensuing analysis, we now set up a polar coordinate system in which the origin is at the AP and the scheduled DL user is at $x_d = (r, 0)$. Therefore, according to the bipolar poisson model, we have $\ell(x_u) = (r^2 + d^2 - 2rd\cos\theta)^{-\alpha/2}$. In the following, we will need the exact knowledge of the spatial distribution of the $\ell(x_u)$ in terms of r and θ. Since we assume that nearest DL user is scheduled for downlink transmission, x_d denotes the distance between the AP and the nearest DL user. Therefore, the probability distribution function (pdf) of the nearest distance x_d for the homogeneous PPP Φ_d with intensity λ_d is given by [19]

$$f_r(r) = 2\pi\lambda_d r e^{-\lambda_d \pi r^2}, \qquad r \geq 0. \tag{3}$$

Moreover, angular distribution is uniformly distributed over $[0 \ 2\pi]$ i.e., $f_\theta(\theta) = 1/2\pi$.

III. PERFORMANCE ANALYSIS

In this section, we derive analytical outage probability and sum rate expressions. First, we obtain the cumulative distribution function (cdf) of the SINRs, $\mathsf{SINR_d}$ and $\mathsf{SINR_a}$. Next exploiting the cdf result, the outage probability and sum rate are derived.

A. The SINR cdfs at the AP and DL User

The cdf of the $\mathsf{SINR_a}$ and the $\mathsf{SINR_d}$ are respectively expressed by

$$F_{\mathsf{SINR}_i}(z) = 1 - \Pr(\mathsf{SINR}_i \geq z), \tag{4}$$

for $i \in \{a, d\}$ and $z \geq 0$, where $\Pr(\cdot)$ denotes the probability. We now proceed to derive exact expressions for $F_{\mathsf{SINR}_a}(z)$ and $F_{\mathsf{SINR}_d}(z)$, respectively.

Uplink Transmission: Using (4), the $\mathsf{SINR_a}$ cdf can be written as

$$F_{\mathsf{SINR}_a}(z) = 1 - \mathbb{E}_{r,\theta}\left\{\Pr\left(h_{ua} \geq \frac{z}{P_u \ell(x_u)}[P_a h_{aa} + \sigma_n^2]\Big| h_{aa}\right)\right\}$$

$$= 1 - \mathbb{E}_{r,\theta}\left\{\frac{e^{-z\frac{\sigma_n^2}{P_u}(r^2 + d^2 - 2rd\cos\theta)^{\alpha/2}}}{1 + z\frac{P_a}{P_u}\sigma_{aa}^2(r^2 + d^2 - 2rd\cos\theta)^{\alpha/2}}\right\}, \tag{5}$$

where the second equality in (5) is due to $h_{aa} \sim \exp(1/\sigma_{aa}^2)$. With the aid of the pdfs for r and θ, we can express $F_{\mathsf{SINR}_a}(z)$ as $F_{\mathsf{SINR}_a}(z) =$

$$1 - \lambda_d \int_0^{R_c} \int_0^{2\pi} \frac{re^{-\lambda_d \pi r^2} e^{-\frac{z\sigma_n^2}{P_u}(r^2 + d^2 - 2rd\cos\theta)^{\frac{\alpha}{2}}}}{1 + z\frac{P_a}{P_u}\sigma_{aa}^2(r^2 + d^2 - 2rd\cos\theta)^{\frac{\alpha}{2}}} d\theta dr. \tag{6}$$

In general, the double integral in (6) does not admit a simple analytical solution for an arbitrary value of α. However, the cdf can be conveniently evaluated using numerical integration. The following propositions characterize $F_{\mathsf{SINR}_a}(z)$ for

the interference-limited scenario with $\sigma_n^2 = 0$ and special cases[1]; $\alpha = 2$ and $\alpha = 4$.

Proposition 1. *The cdf of* $\mathsf{SINR_a}$, *for* $\alpha = 2$ *is given by*

$$F_{\mathsf{SINR_a}}(z) = 1 - \frac{P_u}{P_a} \frac{8\pi\lambda_d}{z\sigma_{aa}^2} \sum_{k=0}^{\infty} \frac{(-2\pi\lambda_d c)^k}{\Gamma(k+1)} \sqrt{c} \left(\frac{b-\sqrt{c}\varrho}{c-b^2}\right)^{k+1}$$

$$\times F_1\left(k+1;k+1,k+1;k+2;\frac{b-\sqrt{c}\varrho}{b+\sqrt{c}},\frac{b-\sqrt{c}\varrho}{b-\sqrt{c}}\right), \quad (7)$$

where $c = \left(\frac{P_u}{P_a}\frac{1}{z\sigma_{aa}^2}+d^2\right)^2$, $b = \frac{P_u}{P_a}\frac{1}{z\sigma_{aa}^2}-d^2$, $\varrho = (\sqrt{R_c^4+bR_c^2+c}-\sqrt{c})/R_c^2$, $\Gamma(\cdot)$ *is the Gamma function [20, Eq. (8.310.1)], and* $F_1(\cdot;\cdot,\cdot;\cdot;\cdot,\cdot)$ *is the Appell hypergeometric function [21, Eq. (5.8.5)].*

Proof: Following (6), the $F_{\mathsf{SINR_d}}(z)$ corresponding to $\alpha = 2$ and $\sigma_n^2 = 0$ is given by $F_{\mathsf{SINR_a}}(z) =$

$$1 - \frac{P_u}{P_a}\frac{1}{z\sigma_{aa}^2}\int_0^{R_c}\int_0^{2\pi}\frac{\lambda_d r e^{-\lambda_d\pi r^2}}{\frac{P_u}{P_a}\frac{1}{z\sigma_{aa}^2}+r^2+d^2-2rd\cos\theta}d\theta dr.$$

With the help of [20, Eq. (3.661.4)], and next making the change of variable $r^2 = \upsilon$, we obtain

$$F_{\mathsf{SINR_a}}(z) = 1 - \frac{P_u}{P_a}\frac{\pi\lambda_d}{z\sigma_{aa}^2}\int_0^{R_c^2}\frac{e^{-\lambda_d\pi\upsilon}}{\sqrt{\upsilon^2+2b\upsilon+c}}d\upsilon. \quad (8)$$

To the best of our knowledge, the integral in (8) does not admit a closed-form solution. In order to proceed, we use Taylor series representation [20, Eq. (1.211.1)] for term $e^{-\lambda_d\pi\upsilon}$, and write

$$F_{\mathsf{SINR_a}}(z) = 1 - \frac{P_u}{P_a}\frac{\pi\lambda_d}{z\sigma_{aa}^2} \quad (9)$$

$$\times \sum_{k=0}^{\infty}\frac{(-\lambda_d\pi)^k}{k!}\int_0^{R_c^2}\frac{\upsilon^k}{\sqrt{\upsilon^2+2b\upsilon+c}}d\upsilon.$$

A change of variable $\sqrt{\upsilon^2+2b\upsilon+c} = \upsilon t + \sqrt{c}$, and after some manipulations, (9) can be expressed as

$$F_{\mathsf{SINR_a}}(z) = 1 - \frac{P_u}{P_a}\frac{4\pi\lambda_d}{z\sigma_{aa}^2}$$

$$\times \sum_{k=0}^{\infty}\frac{(-\lambda_d\pi)^k}{k!}\int_{\frac{b}{\sqrt{c}}}^{\varrho}\frac{(b-\sqrt{c}t)^k}{(t^2-1)^{k+1}}dt. \quad (10)$$

Finally, using [21, Eq. (5.8.5)], we get the desired result given in (7). ∎

Proposition 2. *The cdf of* $\mathsf{SINR_a}$ *for* $\alpha = 4$ *is lower bounded as*

$$F_{\mathsf{SINR_a}}(z) > 1 - \sum_{k=0}^{\infty}\frac{(-1)^k(\lambda_d\pi R_c^2)^{k+1}}{\Gamma(k+2)}$$

$$\times {}_2F_1\left(1,\frac{k+1}{2},\frac{k+1}{2}+1,-z\sigma_{aa}^2\frac{P_a}{P_u}R_c^4\right), \quad (11)$$

where ${}_2F_1(\cdot,\cdot;\cdot;\cdot)$ *denotes the Gauss hypergeometric function defined in [20, Eq. (9.111)].*

Proof: Following (6), the $F_{\mathsf{SINR_a}}(z)$ corresponding to $\alpha = 4$ and $\sigma_n^2 = 0$ can be written as

$$F_{\mathsf{SINR_a}}(z) = 1 - \frac{1}{z}\frac{\lambda_d P_u}{\sigma_{aa}^2 P_a} \quad (12)$$

$$\times\int_0^{R_c}\int_0^{2\pi}\frac{re^{-\lambda_d\pi r^2}}{\frac{P_u}{P_a}\frac{1}{z\sigma_{aa}^2}+(r^2+d^2-2rd\cos\theta)^2}d\theta dr.$$

By using [20], the inner integral can be obtained as

$$F_{\mathsf{SINR_a}}(z) = 1 - \frac{\sqrt{2}\pi}{z}\frac{\lambda_d P_u}{\sigma_{aa}^2 P_a} \quad (13)$$

$$\times\int_0^{R_c}\frac{re^{-\lambda_d\pi r^2}}{\sqrt{c_2(r)+\sqrt{c_4(r)c_0(r)}}}\left[\frac{1}{\sqrt{c_0(r)}}+\frac{1}{\sqrt{c_4(r)}}\right]dr,$$

where $c_0(r) = b_0(r) - b_1(r) + b_2(r)$, $c_2(r) = b_0(r) - b_2(r)$, and $c_4(r) = b_0(r) + b_1(r) + b_2(r)$, with $b_0(r) = P_u/(P_a z\sigma_{aa}^2) + (r^2+d^2)^2$, $b_1(r) = 4rd(r^2+d^2)$, and $b_2(r) = 4r^2 d^2$. The integral in (13) cannot be calculated analytically. However, we can simplify the above integral in the case of $d = 0$. Hence, after a simple substitution $r^2 = \upsilon$, (13) can be written as

$$F_{\mathsf{SINR_a}}(z) > 1 - \frac{\pi}{z}\frac{\lambda_d P_u}{\sigma_{aa}^2 P_a}\int_0^{R_c^2}\frac{e^{-\lambda_d\pi\upsilon}}{\upsilon^2+\frac{P_u}{P_a}\frac{1}{z\sigma_{aa}^2}}d\upsilon. \quad (14)$$

In order to simplify (14), we adopt a series expansion of the exponential term. Substituting the series expansion of $e^{-\lambda_d\pi\upsilon}$ into the (14) yields

$$F_{\mathsf{SINR_a}}(z) > 1 - \frac{1}{z}\frac{P_u}{\sigma_{aa}^2 P_a}\times$$

$$\sum_{k=0}^{\infty}\frac{(-\lambda_d\pi)^{k+1}}{k!}\int_0^{R_c^2}\frac{\upsilon^k}{\upsilon^2+\frac{P_u}{P_a}\frac{1}{z\sigma_{aa}^2}}d\upsilon. \quad (15)$$

Let us denote $\beta = \frac{P_u}{P_a}\frac{1}{z\sigma_{aa}^2}$. By making the change of variable $(\upsilon/R_c^2)^2 = t$, we obtain

$$F_{\mathsf{SINR_a}}(z) > 1 - \sum_{k=0}^{\infty}\frac{(-\lambda_d\pi R_c^2)^{k+1}}{2k!}\int_0^1\frac{t^{\frac{k-1}{2}}}{1+\frac{R_c^4}{\beta}t}dt. \quad (16)$$

Now with the help of [20, Eq. (9.111)] the integral in (16) can be solved to yield (11). ∎

Downlink Transmission: Using (1) and (4), the cdf of $\mathsf{SINR_d}$ can be written as

$$F_{\mathsf{SINR_d}}(z) = 1 - \mathbb{E}_{I_{d,u}}\left\{\Pr\left(P_a h_{ad}r^{-\alpha}\geq z[I_{d,u}+\sigma_n^2]\right)|r\right\},$$

$$= 1 - \mathbb{E}_{I_{d,u}}\left\{e^{-\frac{z}{P_a}r^\alpha[I_{d,u}+\sigma_n^2]}|r\right\}. \quad (17)$$

Note that in our system model the randomness of the $I_{d,u}$ is due to the fading power envelope h_{du}. As such, $F_{\mathsf{SINR_d}}(z)$ can be written as

$$F_{\mathsf{SINR_d}}(z) = 1 - \mathbb{E}_r\left\{e^{-\frac{z}{P_a}\sigma_n^2 r^\alpha}\int_0^\infty e^{-\left(\frac{r}{d}\right)^\alpha\frac{P_u}{P_a}zx}e^{-x}dx\right\},$$

$$= 1 - 2\pi\lambda_d\int_0^{R_c}r\frac{e^{-z\frac{\sigma_n^2}{P_a}r^\alpha}e^{-\lambda_d\pi r^2}}{1+\left(\frac{r}{d}\right)^\alpha\frac{P_u}{P_a}z}dr. \quad (18)$$

Eq. (18) does not have a closed-form solution. However, an expression for $F_{\mathsf{SINR_d}}(z)$ can be derived in the interference-limited case in Proposition 3.

Proposition 3. *The cdf of* $\mathsf{SINR_d}$, *can be expressed as*

$$F_{\mathsf{SINR_d}}(z) = 1 - \sum_{k=0}^{\infty}\frac{(-1)^k(\lambda_d\pi R_c^2)^{k+1}}{\Gamma(k+2)} \quad (19)$$

$$\times {}_2F_1\left(1,\frac{2(k+1)}{\alpha},\frac{2(k+1)}{\alpha}+1,-z\frac{P_u}{P_a}\left(\frac{R_c}{d}\right)^\alpha\right).$$

Proof: The proof, similar to *Proposition 2*, is omitted. ∎

B. Outage Probability

The outage probability is an important quality-of-service metric defined as the probability that SINR_i, $i \in \{a, d\}$, drops

---

[1]Note that $\alpha = 2$ and $\alpha = 4$ correspond to free space propagation and typical rural areas, respectively, and constitute useful bounds for practical propagation conditions.

below an acceptable SINR threshold, γ_{th}. We now present the following corollaries to establish the DL and UL user outage probability valid in the interference-limited case (i.e., $\sigma_n^2 = 0$).

Corollary 1. *The UL user outage probability with $\alpha = 2$ is given by substituting $z = \gamma_{th}$ into (7). Moreover, for $\alpha = 4$, the outage probability is lower bounded by substituting $z = \gamma_{th}$ into (11).*

Corollary 2. *The UL user outage probability is given by substituting $z = \gamma_{th}$ into (19).*

C. Achievable Sum Rate

The achievable sum rate with simultaneous UL/DL transmission can be written as

$$R_{\mathsf{FD}} = R_{\mathsf{a}} + R_{\mathsf{d}}, \tag{20}$$

where $R_{\mathsf{a}} = \mathbb{E}\{\log_2[1 + \mathsf{SINR_a}]\}$ and $R_{\mathsf{d}} = \mathbb{E}\{\log_2[1 + \mathsf{SINR_d}]\}$ are the spatial average capacity of the UL ($x_{\mathsf{u}} \to$ AP) and DL (AP $\to x_{\mathsf{d}}$), respectively.

Note that since $\mathbb{E}\{X\} = \int_{t=0}^{\infty} \Pr(X > t)dt$ for a nonnegative random variable X, the spatial average capacity can be written as

$$R_i = \int_0^{\infty} [1 - F_{\mathsf{SINR}_i}(\epsilon_t)]\, dt. \tag{21}$$

where $i \in \{\mathsf{a}, \mathsf{d}\}$ and $\epsilon_t = 2^t - 1$.

Uplink Transmission: By substituting (5) into (21), the exact average capacity of the UL user can be written as

$$R_{\mathsf{a}} = \int_0^{\infty} \int_0^{R_c} \int_0^{2\pi} \tag{22}$$
$$\frac{2\pi\lambda_{\mathsf{d}} r e^{-\epsilon_t \frac{\sigma_n^2}{P_{\mathsf{u}}}(r^2 + d^2 - 2rd\cos\theta)^{\alpha/2}} e^{-\lambda_{\mathsf{d}}\pi r^2}}{1 + \epsilon_t \frac{P_{\mathsf{a}}}{P_{\mathsf{u}}}\sigma_{\mathsf{aa}}^2 (r^2 + d^2 - 2rd\cos\theta)^{\alpha/2}} dr d\theta dt.$$

This integral cannot be solved in closed-form. Therefore, we now turn our attention into deriving the average capacity of the UL user with the interference-limited assumption and $\alpha = 2, 4$.

Corollary 3. *Plugging (7) into (21), the spatial average capacity of the UL user for $\alpha = 2$ is given by*

$$R_{\mathsf{a}} = \frac{8\pi\lambda_{\mathsf{d}}}{\sigma_{\mathsf{aa}}^2 \log 2} \frac{P_{\mathsf{u}}}{P_{\mathsf{a}}} \sum_{k=0}^{\infty} \frac{(-2\pi\lambda_{\mathsf{d}})^k}{\Gamma(k+1)} \int_0^{\infty} \frac{c^{k+\frac{1}{2}}}{z(z+1)} \left(\frac{b - \sqrt{c}\varrho}{c - b^2}\right)^{k+1}$$
$$\times F_1\left(k+1; k+1, k+1; k+2; \frac{b - \sqrt{c}\varrho}{b + \sqrt{c}}, \frac{b - \sqrt{c}\varrho}{b - \sqrt{c}}\right) dz. \tag{23}$$

Proposition 4. *For $\alpha = 4$, the spatial average capacity of the UL user is upper bounded by*

$$R_{\mathsf{a}} < \frac{2}{\log 2} \sum_{k=0}^{\infty} \frac{(-1)^k (\lambda_{\mathsf{d}}\pi R_c^2)^{k+1}}{(k+1)\Gamma(k+2)}$$
$$\times G_{3\ 3}^{2\ 3}\left(\frac{P_{\mathsf{a}}}{P_{\mathsf{u}}} R_c^4 \sigma_{\mathsf{aa}}^2 \,\bigg|\, \begin{matrix} 0, 1 - \frac{k+1}{2}, 0 \\ 0, 0, -\frac{k+1}{2} \end{matrix}\right), \tag{24}$$

where $G_{pq}^{mn}\left(z \,\big|\, \begin{smallmatrix} a_1 \cdots a_p \\ b_1 \cdots b_q \end{smallmatrix}\right)$ denotes the Meijer G-function defined in [20, Eq. (9.301)].

Proof: By substituting the lower bound of $F_{\mathsf{SINR_a}}(\cdot)$ from Proposition 2 into (21), and applying the transformation $y = 2^t - 1$, an upper bound for the average capacity of the UL

user can be derived as

$$R_{\mathsf{a}} < \frac{1}{\log 2} \sum_{k=0}^{\infty} \frac{(-1)^k (\lambda_{\mathsf{d}}\pi R_c^2)^{k+1}}{\Gamma(k+2)}$$
$$\times \underbrace{\int_0^{\infty} \frac{1}{y+1} {}_2F_1\left(1, \frac{k+1}{2}, \frac{k+1}{2} + 1, -\sigma_{\mathsf{aa}}^2 \frac{P_{\mathsf{a}}}{P_{\mathsf{u}}} R_c^4 y\right) dy}_{\mathcal{I}},$$

where the integral, $\mathcal{I}$ can be expressed [22, Eq. (17)] in terms of the tabulated Meijer G-function as

$$\mathcal{I} = \frac{2}{k+1} \int_0^{\infty} G_{11}^{11}\left(y \,\bigg|\, \begin{matrix} 0 \\ 0 \end{matrix}\right)$$
$$\times G_{22}^{12}\left(\frac{P_{\mathsf{a}}}{P_{\mathsf{u}}} R_c^4 \sigma_{\mathsf{aa}}^2 y \,\bigg|\, \begin{matrix} 0, 1 - \frac{k+1}{2} \\ 0, -\frac{k+1}{2} \end{matrix}\right) dy. \tag{25}$$

The above integral can be solved with the help of [22, Eq. (21)] to yield the desired result in (24). ∎

Downlink Transmission: By plugging (18) into (21), exact average capacity of the DL user can be written as

$$R_{\mathsf{d}} = 2\pi\lambda_{\mathsf{d}} \int_0^{\infty} \int_0^{\infty} \frac{re^{-\epsilon_t \frac{\sigma_n^2}{P_{\mathsf{a}}} r^{\alpha}} e^{-\lambda_{\mathsf{d}}\pi r^2}}{1 + \left(\frac{r}{d}\right)^{\alpha} \frac{P_{\mathsf{u}}}{P_{\mathsf{a}}} \epsilon_t} dr. \tag{26}$$

Moreover, for the interference-limited case (i.e., $\sigma_n^2 = 0$), using the cdf in (19), Proposition 5 presents the average capacity of the DL user.

Proposition 5. *The spatial average capacity of the DL user in the interference-limited case is expressed as*

$$R_{\mathsf{d}} = \frac{\alpha}{2} \sum_{k=0}^{\infty} \frac{(-1)^k (\lambda_{\mathsf{d}}\pi R_c^2)^{k+1}}{(k+1)\Gamma(k+2)}$$
$$\times G_{3\ 3}^{2\ 3}\left(\frac{P_{\mathsf{u}}}{P_{\mathsf{a}}} \left(\frac{R_c}{d}\right)^{\alpha} \,\bigg|\, \begin{matrix} 0, 1 - \frac{2(k+1)}{\alpha}, 0 \\ 0, 0, -\frac{2(k+1)}{\alpha} \end{matrix}\right). \tag{27}$$

Proof: The proof, similar to *Proposition 4*, is omitted. ∎

Asymptotic Analysis: In order to present further insights into the system performance, we now investigate the asymptotic outage probability and achievable rate by neglecting the interference terms in the UL and DL SINRs. Therefore, with negligible LI effect, one can omit the term $P_{\mathsf{a}} h_{\mathsf{aa}}$ in (2). Finally, the cdf of the SNR in the special case of $\alpha = 2$ can be obtained as

$$F_{\mathsf{SNR_a}}(z) = 1 - \left(1 + \frac{z}{\psi_{\mathsf{u}}}\right)^{-1} e^{-\frac{\lambda_{\mathsf{d}}\pi d^2}{1 + \frac{\psi_{\mathsf{u}}}{z}}}, \tag{28}$$

where $\psi_{\mathsf{u}} = \frac{P_{\mathsf{u}}}{\sigma_n^2}\lambda_{\mathsf{d}}\pi$. The asymptotic outage of the UL transmission can be determined by substituting $z = \gamma_{th}$ into (28). Furthermore, the corresponding asymptotic spatial average capacity of the UL user is

$$R_{\mathsf{a}} = \frac{1}{\log 2} \left(\frac{1}{\psi_{\mathsf{u}}} - 1\right)^{-1} e^{-\frac{\lambda_{\mathsf{d}}\pi d^2}{\psi_{\mathsf{u}}}}$$
$$\times \left(\mathrm{Ei}\left(\frac{\lambda_{\mathsf{d}}\pi d^2}{1 - \psi_{\mathsf{u}}}\right) - \mathrm{Ei}\left(\frac{\psi_{\mathsf{u}}\lambda_{\mathsf{d}}\pi d^2}{1 - \psi_{\mathsf{u}}}\right)\right), \tag{29}$$

where $\mathrm{Ei}(\cdot)$ is the exponential integral function defined in [20, Eq. (8.211.1)]. Similarly, by neglecting the term $P_{\mathsf{u}} h_{\mathsf{ud}} \ell(x_{\mathsf{u}} - x_{\mathsf{d}})$ in (1), a valid assumption for $P_{\mathsf{u}} d^{-\alpha} \ll 1$,
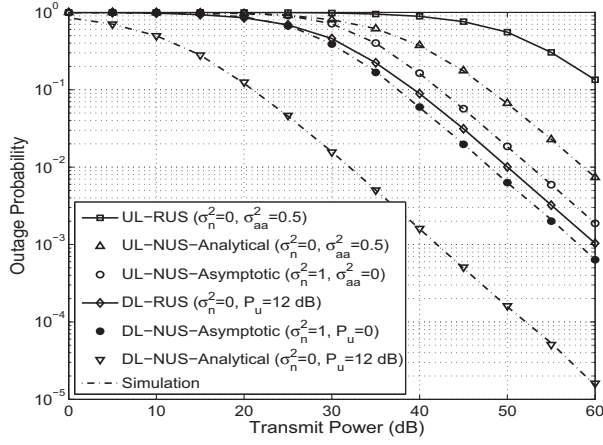
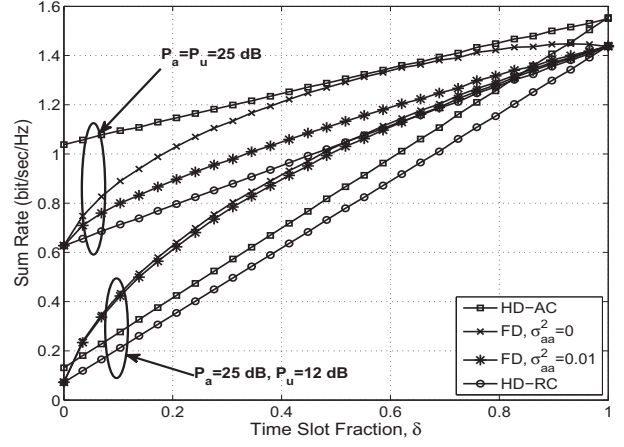Fig. 1. Outage performance of the DL and UL user for nearest user selection (NUS) and random user selection (RUS) ($d = 25$ m and $\gamma_{th} = 3$ dB)

Fig. 2. Average sum rate versus δ for the FD (FD) and half-dulpex (HD) AP ($\alpha = 2$, and $d = 25$ m).

we obtain

$$
F_{\mathsf{SNR_d}}(z) = \begin{cases} 1 - \left(1 + \frac{z\lambda_{\mathsf{d}}\pi}{\psi_{\mathsf{d}}}\right)^{-1} & \alpha = 2, \\ 1 - \sqrt{\frac{\psi_{\mathsf{d}}}{2z}} e^{\frac{\psi_{\mathsf{d}}}{8z}} D_{-1}\left(\sqrt{\frac{\psi_{\mathsf{d}}}{2z}}\right) & \alpha = 4 \end{cases} \tag{30}
$$

where $\psi_{\mathsf{d}} = \frac{P_{\mathsf{a}}}{\sigma_n^2}(\lambda_{\mathsf{d}}\pi)^2$ and $D_{-1}(\cdot)$ denotes a Parabolic cylinder function [20, Eq. (9.241.2)]. Accordingly, the DL user asymptotic outage probability can be readily obtained by substituting $z = \gamma_{th}$ into (30). Moreover, the corresponding rates are given by

$$
R_{\mathsf{d}} = \frac{1}{\log 2} \begin{cases} \left(\frac{\lambda_{\mathsf{d}}\pi}{\psi_{\mathsf{d}}} - 1\right)^{-1} \log\left(\frac{\lambda_{\mathsf{d}}\pi}{\psi_{\mathsf{d}}}\right) & \alpha = 2, \\ \int_0^\infty \frac{1}{z+1}\sqrt{\frac{\psi_{\mathsf{d}}}{2z}} e^{\frac{\psi_{\mathsf{d}}}{8z}} D_{-1}\left(\sqrt{\frac{\psi_{\mathsf{d}}}{2z}}\right) dz & \alpha = 4. \end{cases} \tag{31}
$$

D. Half-Duplex Mode

In this subsection, we compare the performance of the HD and FD modes of operation at the AP. In the HD mode of AP operation, AP employs orthogonal time slots to serve the DL and UL user, respectively. In order to keep our comparisons fair, we consider *"antenna conserved"* (AC) and *"RF-chain conserved"* (RC) scenarios. Under AC condition, the total number of antennas used by the HD AP and FD AP is kept identical. However, the number of radio frequency (RF) chains employed by the HD AP is twice that of the FD AP [6] and hence former system would be a costly option. Under RC condition, the total number RF chains used is same for the HD and FD modes. Therefore, in any transmission (UL or DL), the HD AP only uses a single antenna under the RC condition, while it uses two antennas under the AC condition. The average sum rate under the RC condition can be expressed as

$$
R_{\mathsf{HD}}^{\mathsf{RC}} = \delta\mathbb{E}\left\{\log_2\left(1 + \mathsf{snr_d}\ell(x_{\mathsf{d}})|h_{\mathsf{a,d}}|^2\right)\right\} + (1 - \delta)\mathbb{E}\left\{\log_2\left(1 + \mathsf{snr_u}\ell(x_{\mathsf{u}})|h_{\mathsf{d,a}}|^2\right)\right\}, \tag{32}
$$

where δ ($0 < \delta < 1$) is a fraction of the time slot duration of T, used for DL transmission, $\mathsf{snr_d} = P_{\mathsf{a}}^{\mathsf{HD}}/\sigma_n^2$, and $\mathsf{snr_u} = P_{\mathsf{u}}^{\mathsf{HD}}/\sigma_n^2$.

Under the AC condition, using the weight vector $\boldsymbol{w}_{\mathsf{MRC}} = \boldsymbol{h}_{\mathsf{d,a}}^H$ for the maximum ratio combining (MRC) receiver, and the maximum ratio transmission (MRT) precoding vector $\boldsymbol{w}_{\mathsf{MRT}} = \frac{\boldsymbol{h}_{\mathsf{a,d}}^H}{\|\boldsymbol{h}_{\mathsf{a,d}}\|}$, the average achievable rate can be obtained

as

$$
R_{\mathsf{HD}}^{\mathsf{AC}} = \delta\mathbb{E}\left\{\log_2\left(1 + \frac{\mathsf{snr_d}}{2}\ell(x_{\mathsf{d}})\|\boldsymbol{h}_{\mathsf{a,d}}\|^2\right)\right\} + (1 - \delta)\mathbb{E}\left\{\log_2\left(1 + \mathsf{snr_u}\ell(x_{\mathsf{u}})\|\boldsymbol{h}_{\mathsf{d,a}}\|^2\right)\right\}. \tag{33}
$$

IV. NUMERICAL RESULTS AND DISCUSSION

Here, we investigate the system performance and confirm the derived analytical results through comparison with Monte Carlo simulations. We evaluate the performance in a cell of radius $R_c = 200$ m and for $\lambda_{\mathsf{d}} = 1 \times 10^{-3}$ node/m². Moreover, with curves shown in Figs. 3-5, we assume that the total power of the AP and UL user for FD and HD modes is the same.

Fig. 1 shows the outage probability versus SNR for the nearest DL user (to the AP) and UL user for $\alpha = 2$, $d = 25$ m and $\gamma_{th} = 3$ dB. In this figure, the X-axis indicates the power of the transmitter (i.e., AP for DL and UL user for UL). The outage probability of the RUS scheme is also included as a benchmark comparison. The 'Analytical' curves are plotted from (7) and (19) with $z = \gamma_{th}$, for nearest UL user and DL user, respectively, which clearly match the Monte Carlo simulated curves. As expected, we see that the nearest user selection (NUS) scheme outperforms the RUS scheme. In addition, the 'Asymptotic' curves plotted from (28) and (30) tightly converge to the simulation values.

In Fig. 2 we compare the average sum rate as a function of δ for the FD and HD operation and for two different values of σ_{aa}^2. We assume same total energy consumption for both FD and HD operation and plot the sum rate for two different power constraints $(P_{\mathsf{a}}, P_{\mathsf{u}}) = (25 \text{ dB}, 25 \text{ dB})$ (symmetric) and $(P_{\mathsf{a}}, P_{\mathsf{u}}) = (25 \text{ dB}, 12 \text{ dB})$ (asymmetric). In particular, numerical results lead to the following conclusions: 1) As expected, the sum rate under the RC condition is worse than those of other scenarios. 2) In the asymmetric case, FD operation outperforms HD within the practical range of δ. However, in the symmetric case, AC condition achieves the best performance even in case of perfect LI cancellation (i.e., $\sigma_{\mathsf{aa}}^2 = 0$). 3) The symmetric case is more vulnerable to the LI power (Please see Fig. 4).

In Fig. 3, we present the average sum rate (with $\delta = 0.5$ and $\sigma_{\mathsf{aa}}^2 = 0.1$) versus the distance d between the UL and DL user achieved by the FD and HD modes of operation. There are two main observations that can be extracted from
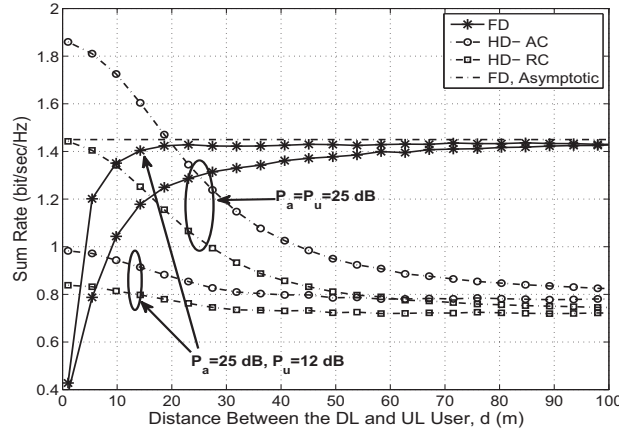
Fig. 3. Average sum rate versus d the FD and half-dulpex (HD) AP ($\alpha = 2$, $\delta = 0.5$, and $\sigma_{aa}^2 = 0.1$).
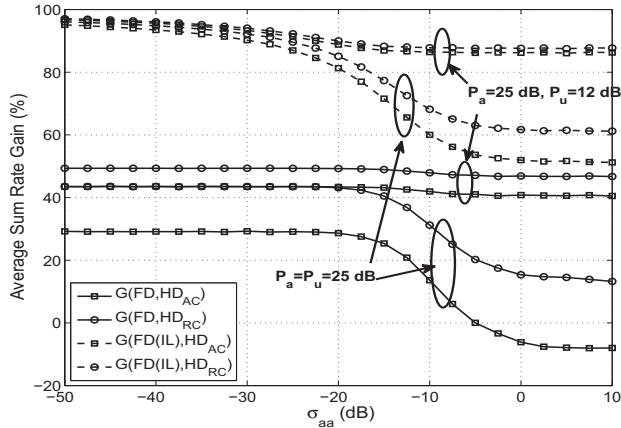

Fig. 4. Average sum rate gain of the system ($\alpha = 2$, $d = 25$ m, and $\delta = 0.5$).

this figure. First, the sum rate shows the opposite behaviors in FD and HD modes as d increases. This result can be explained as follows. Notice that when d increases the inter user interference between the DL and UL user decreases and thus $\mathsf{SINR_d}$ and consequently the average sum rate of the FD system increases. On the other hand, the sum rate of the HD operation is inversely proportional to d. Therefore, increasing d, reduces the sum rate. Secondly, as d increases the average sum rate of the FD system converges to the sum of asymptotic rate in (29) and (31).

In Fig. 4 we plot the average sum rate gain, which is defined as $G(\mathsf{FD}, \mathsf{HD}_i) = (R_{\mathsf{FD}} - R_{\mathsf{HD}}^i)/R_{\mathsf{FD}}$ versus σ_{aa} and for $d = 25$ m and $\delta = 0.5$. The sum rate gain of the interference-limited FD system is also included for comparison (dashed line curves). A general observation is that FD significantly outperforms the HD counterpart when LI is substantially suppressed. However, when $\sigma_{aa} \geq -5$ dB, the AC-HD system outperforms the FD system (symmetric power case). Moreover, the symmetric power case is more sensitive to the LI effect.

V. CONCLUSION

We have analyzed the performance of a wireless network scenario where a FD AP is communicating with spatially random HD user terminals in the downlink and uplink channels simultaneously. We derived the outage probability and achievable sum rate of the system, considering the impact of the LI channel and inter user interference. Then, we

compared the performance of the FD and HD modes of operations for the same total power budget. We found that even if the LI cancellation is imperfect, FD transmissions with different transmit power levels at the AP and the UL user can achieve significant performance gains as compared to the HD mode of operation.

REFERENCES

[1] D. W. Bliss, P. A. Parker, and A. R. Margetts, "Simultaneous transmission and reception for improved wireless network performance," in *Proc. IEEE Workshop Statist. Signal Process.*, Madison, WI, Aug. 2007, pp. 478–482.

[2] A. Sabharwal, P. Schniter, D. Guo, D. W. Bliss, S. Rangarajan, and R. Wichman, "In-band full-duplex wireless: Challenges and opportunities," *IEEE J. Sel. Areas Commun.*, vol. 32, pp. 1637–1652, Sep. 2014.

[3] M. Duarte, "Full-duplex wireless: Design, implementation and characterization," Ph.D. dissertation, Dept. Elect. and Computer Eng., Rice University, Houston, TX, 2012.

[4] T. Riihonen, S. Werner, R. Wichman, and E. B. Zacarias, "On the feasibility of full-duplex relaying in the presence of loop interference," in *Proc.10th IEEE Workshop on Signal Process. Adv. Wireless Commun.*, Perugia, Italy, June 2009, pp. 275–279.

[5] T. Riihonen, S. Werner, and R. Wichman, "Mitigation of loopback self-interference in full-duplex MIMO relays," *IEEE Trans. Signal Process.*, vol. 59, pp. 5983–5993, Dec. 2011.

[6] E. Aryafar, M. A. Khojastepour, K. Sundaresan, S. Rangarajan, and M. Chiang, "MIDU: Enabling MIMO full duplex," in *Proc. 18th Intl. Conf. Mobile Computing and Networking (ACM Mobicom '12)*, New York, NY, Aug. 2012, pp. 257–268.

[7] D. Bharadia and S. Katti, "Full-duplex MIMO radios," in *Proc. 11th USENIX Symp. Networked Syst. Design and Implementation (NSDI '14)*, Seattle, WA, Apr. 2014, pp. 359–372.

[8] H. Q. Ngo, H. A. Suraweera, M. Matthaiou, and E. G. Larsson, "Multipair full-duplex relaying with massive arrays and linear processing," *IEEE J. Sel. Areas Commun.*, vol. 32, pp. 1721–1737, Sep 2014.

[9] S. Goyal, P. Liu, S. Hua, and S. S. Panwar, "Analyzing a full-duplex cellular system," in *Proc. 47th Annual Conf. on Information Sciences and Systems (CISS)*, Baltimore, MD, Mar. 2013, pp. 1–6.

[10] M. Vehkaperä, M. Girnyk, T. Riihonen, R. Wichman, and L. Rasmussen, "On achievable rate regions at large-system limit in full-duplex wireless local access," in *Proc. 1st Intl. Black Sea Conf. Commun. and Networking (BlackSeaCom)*, Batumi, Georgia, July 2013, pp. 7–11.

[11] B. Yin, M. Wu, C. Studer, J. R. Cavallaro, and J. Lilleberg, "Full-duplex in large-scale wireless systems," in *Proc. Asilomar Conf. Signals, Systems and Computers (ASILOMAR 2013)*, Pacific Grove, CA, Nov. 2013, pp. 1623–1627.

[12] A. Sahai, S. Diggavi, and A. Sabharwal, "On uplink/downlink full-duplex networks," in *Proc. Asilomar Conf. Signals, Systems and Computers (ASILOMAR 2013)*, Pacific Grove, CA, Nov. 2013, pp. 14–18.

[13] S. Goyal, P. Liu, S. S. Panwar, R. A. DiFazio, R. Yang, J. Li, and E. Bala, "Improving small cell capacity with common-carrier full duplex radios," in *Proc. IEEE Intl. Conf. Commun. (ICC 2014)*, Sydney, Australia, June 2014, pp. 4987–4993.

[14] D. Nguyen, L.-N. Tran, P. Pirinen, and M. Latva-aho, "Precoding for full duplex multiuser MIMO systems: Spectral and energy efficiency maximization," *IEEE Trans. Signal Process.*, vol. 61, pp. 4038–4050, Aug. 2013.

[15] F. Baccelli and B. Blaszczyszyn, *Stochastic Geometry and Wireless Networks. NOW: Foundations and Trends in Networking*, 2010.

[16] J. G. Andrews, "Seven ways that HetNets are a cellular paradigm shift," *IEEE Commun. Mag.*, vol. 51, pp. 136–144, Mar. 2013.

[17] I. Krikidis, H. A. Suraweera, P. J. Smith, and C. Yuen, "Full-duplex relay selection for amplify-and-forward cooperative networks," *IEEE Trans. Wireless Commun.*, vol. 11, pp. 4381–4393, Dec. 2012.

[18] T. Riihonen, S. Werner, and R. Wichman, "Hybrid full-duplex/half-duplex relaying with transmit power adaptation," *IEEE Trans. Wireless Commun.*, vol. 10, no. 9, pp. 3074–3085, Sep. 2011.

[19] M. Haenggi, "On distances in uniformly random networks," *IEEE Trans. Inf. Theory*, vol. 51, pp. 3584–3586, Oct. 2005.

[20] I. S. Gradshteyn and I. M. Ryzhik, *Table of Integrals, Series and Products*, 7th ed. Academic Press, 2007.

[21] A. Erdelyi, *Higher Transcendental Functions*. New York: McGraw-Hill, 1953, vol. 1.

[22] V. S. Adamchik and O. I. Marichev, "The algorithm for calculating integrals of hypergeometric type functions and its realization in REDUCE system," in *Proc. Int. Conf. Symbolic and Algebraic Comput.*, Tokyo, Japan, 1990, pp. 212 – 224.